Migration of Cr-vacancy clusters and interstitial Cr in α-Fe using the dimer method

D. Chen,[1,2] F. Gao,[2,*] W. Y. Hu,[1] S. Y. Hu,[2] D. Terentyev,[3] X. Sun,[2] H. L. Heinisch,[2] C. H. Henager,[2] and M. A. Khaleel[2]
[1]*Department of Applied Physics, Hunan University, Changsha 410082, China*
[2]*Pacific Northwest National Laboratory, P.O. Box 999, Richland, Washington 99352, USA*
[3]*SCK-CEN, Nuclear Science Institute, Boeretang 200, B-2400 Mol, Belgium*
(Received 2 September 2009; revised manuscript received 24 November 2009; published 1 February 2010)

The migration mechanisms and the corresponding activation energies of Cr-vacancy (Cr-V) clusters and Cr interstitials in α-Fe have been investigated using the dimer and the nudged elastic-band methods. Dimer searches are employed to find the possible transition states of these defects and the lowest-energy paths are used to determine the energy barriers for migration. A substitutional Cr atom can migrate to a nearest-neighbor vacancy through an energy barrier of 0.56 eV but this simple mechanism alone is unlikely to lead to the long-distance migration of Cr unless there is a supersaturated concentration of vacancies in the system. The Cr-vacancy clusters can lead to long-distance migration of a Cr atom that is accomplished by Fe and Cr atoms successively jumping to nearest-neighbor vacancy positions, defined as a self-vacancy-assisted migration mechanism, with the migration energies ranging from 0.64 to 0.89 eV. In addition, a mixed Cr-Fe dumbbell interstitial can easily migrate through Fe lattices, with the migration energy barrier of 0.17, which is lower than that of the Fe-Fe interstitial. The on-site rotation of the Cr-Fe interstitial and Cr atom hopping from one site to another are believed to comprise the dominant migration mechanism. The calculated binding energies of Cr-V clusters are strongly dependent on the size of clusters and the concentration of Cr atoms in clusters.

DOI: 10.1103/PhysRevB.81.064101 PACS number(s): 61.72.Bb, 61.66.Dk, 61.80.Az

I. INTRODUCTION

Point defects and impurities significantly influence the structural and electronic properties of metals and ceramics under irradiation.[1–5] Knowledge of the interactions of microstructures with point defects, such as vacancies and interstitials, is important for developing an understanding of the kinetics and dynamics of microstructural changes in materials under radiation damage conditions. Displacement cascades introduced in the presence of a high concentration of solute atoms such as Cr or Cu atoms in α-Fe can greatly affect the mechanical properties of the materials.[6–9] In Fe-Cr alloys Cr atoms play an important role in radiation-induced evolution of mechanical properties. A concentration of 2–18 % Cr reduces swelling compared to pure Fe[10–12] and a minimum in ductile to brittle transition temperatures appears at about 9% Cr concentration.[13] Alloys containing more than 10% Cr exhibit α-α' phase separation resulting in the formation of the Cr-rich α' phase that is a major cause of hardening of thermally annealed materials,[14,15] indicating the complicated dependence of mechanical properties on Cr concentration. Consequently, interaction of Cr with point defects and the migration mechanism of Cr atoms in Fe-Cr alloys have been studied using *ab initio* calculations[16–18] and molecular-dynamics (MD) methods.[19] These studies revealed that the mixed Cr-Fe dumbbell interstitial can migrate either via a translation or an on-site rotation process so that the Cr atom remains in the defect, or by weakly dissociating the Fe dumbbell atom from the Cr atom, resulting in a substitutional Cr. Also, it is very likely that the mixed Cr-Fe interstitial can be easily trapped and recombines with a nearby vacancy during migration, forming a substitutional Cr and inhibiting its long-distance migration as an interstitial. However, a substitutional Cr atom can also migrate via a vacancy-diffusion mechanism. Indeed, substitutional chromium atoms in bcc Fe have a lower barrier for vacancy-assisted migration than Fe atoms, having a migration energy that is about 0.54 eV lower than the matrix atoms.[18] A supersaturated concentration of vacancies in the system may lead to the long-distance migration of substitutional Cr. Based on this mechanism, the time evolution of vacancy-driven thermal aging was studied using kinetic Monte Carlo techniques[19] and the results showed that initially random Fe-Cr alloys can decomposed into the α' phase. Although these studies provide important information in the formation of Cr defects, the interactions of Cr atoms with point defects and the possible migration mechanisms of Cr atoms in Fe, particularly in the form of Cr-vacancy (Cr-V) clusters, are largely unknown. Thus, computer simulations have been performed to gain insights into the long-distance migration behavior of Cr-vacancy clusters and interstitials in Fe.

The dimer and the nudged elastic band (NEB) methods have been widely used to search for minimum-energy paths (MEPs) of migration of defects and defect clusters in materials. For a given initial and final state of a transition, the minimum-energy path is easily determined using the NEB method. However, there is a very challenging problem how to find the MEP for the transition, if the final state or the mechanism of transition is unknown. Compared to the NEB method, the dimer technique is an especially useful tool for clusters where the lowest-energy final state of its transition is not easily predictable. For example, Gao *et al.*[20] used the dimer method to search for possible transition states of interstitials and interstitial clusters in SiC and α-Fe, addressing the important issue whether or not a migrating interstitials can thermally change migration directions. The dimer method was also employed to study an isolated vacancy, a P-vacancy complex and a P-interstitial defect in Fe and Fe-P systems,[21] as well as revealing that in dilute Fe-P alloys an Fe-P dumbbell is the most mobile defect in Fe-P systems and a P-vacancy complex the least mobile.[22] The dimer method

has also been an indispensible tool for studying the migration of He atoms near and within dislocations and grain boundaries in Fe.[23]

Here, we have employed the dimer method, along with the NEB technique, to search for possible transition states and migration paths of substitutional Cr-V pairs, Cr-V clusters, and Cr-Fe mixed interstitial complexes. In addition, the formation energies and binding energies of Cr-V clusters are determined and compared with those obtained by *ab initio* calculations and empirical interatomic potentials. It is of interest to see that some of the Cr-V clusters are mobile and that their mobilities are strongly enhanced by the presence of additional vacancies. Moreover, these Cr-vacancy clusters can undergo self-long-distance migration without further vacancy assistance, a mechanism that is different from a Cr substitutional atom. The migration energy of a Cr-Fe⟨110⟩ dumbbell interstitial is lower than that of an Fe self-interstitial in α-Fe.

II. COMPUTATIONAL METHOD

The physical properties of point defects, defect clusters, and impurities in Fe have been extensively studied using molecular-dynamics and Monte Carlo methods with empirical interatomic potentials.[24–29] In general, the numerical values of the results depend on the potentials used in the calculations,[30] but for the most part, the relative energies of defect formation and migration are similar, so roughly the same behavior is predicted. In the present study, the pair interaction and the many-body form for Fe were taken from the work of Ackland and Mendelev[31] that provides reasonable descriptions of point defects in comparison to results obtained by performing *ab initio* calculations. This potential has been widely used to simulate cascade damage,[32] helium-defect properties, and clustering[33] and defect evolution in Fe.[34] The interactions between Fe and Cr atoms, as well as the Cr-Cr potential, are described using a two-band second-moment model derived by Olsson *et al.*[19] The Cr-Cr potential is fitted to the cohesive energy, mixing enthalpy, vacancy-formation energy, and interstitial formation energy, whereas the potential for the Fe-Cr interaction is fitted to the lattice parameter of Fe-10Cr, a positive heat of mixing for equimolar composition, the negatively substitutional energy of a single Cr atom in bcc Fe, the crossing point from negative to positive mixing enthalpy and the binding energy of a ⟨110⟩ mixed Cr-Fe dumbbell. These potentials are used to determine the values of the thermodynamic properties of the Fe-Cr system over the whole range of Cr concentration and to calculate point defect properties in Fe-Cr. Furthermore, these potentials have been employed to simulate displacement cascades in Fe-Cr,[35] and have been proven to provide a reasonably good description of the interaction between Cr atoms and point defects in a ferritic matrix. Thus, these potentials should be reliable in the study of migration behaviors and to determine activation energies of Cr-V clusters and Cr-Fe interstitials in Fe.

In this paper, the computational cell consisted of $10a_0 \times 10a_0 \times 10a_0$ unit cells, containing 2000 atoms. Three-dimensional periodic boundary conditions were applied and calculations were carried out at constant volume. The possible transition states and migration paths of the Cr-V clusters and mixed ⟨110⟩ interstitials were investigated by the dimer method[36] and the NEB method,[37] respectively. The dimer method has been described in detail elsewhere[36] so only the central principles are provided here. The dimer method is effective in finding the energies and atom configurations of the saddle points when only the initial state is known, which is different from the nudged elastic-band method where initial and final states need to be known before calculating the transition-energy barrier. The saddle-point search is completed through moving the dimer on the potential-energy surface, from the vicinity of the potential-energy minimum of the initial state up to a saddle point. The potential surface of interest is the $3N$-dimensional surface of all possible configurations of the N atoms in the system. Basins of this surface are stable states while saddle points correspond to the lowest-energy transition points between states, from which the minimum-energy barrier for a transition to take place can be determined. Thus, during the search, each time the dimer is displaced, it is also rotated in order to find the minimum-energy configuration. The dimer separation was set at 1×10^{-3} Å, and the values of the finite difference steps for rotation and translation were 10^{-4} and 10^{-3} Å, respectively. The maximum move distance was set at 0.2 Å and the search was stopped when the maximum force of atoms became less than 0.01 eV/Å. For each initial configuration, we carried out 100 dimer searches with different initial random vectors that have nonzero components only for a 20–30 atom subset of the system near the defect, which allows the system to be displaced from a distribution of nearly equal potential-energy minima in the initial basin.

III. RESULTS AND DISCUSSION

A. Formation and binding properties of Cr-V clusters

The formation energy of a configuration containing n Fe atoms and p Cr atoms is given following the definition in the Refs. 18 and 38, and is given by

$$E_f^{n\mathrm{Fe}+p\mathrm{Cr}} = E_t^{n\mathrm{Fe}+p\mathrm{Cr}} - nE_c^{\mathrm{Fe}} - pE_c^{\mathrm{Cr}}. \quad (1)$$

Here, $E_t^{n\mathrm{Fe}+p\mathrm{Cr}}$ is the total energy of the system containing all the defects while E_c^{Cr} and E_c^{Fe} are the cohesive energy of pure bcc Fe and Cr, respectively. The cohesive energy is obtained from the energy of perfect bcc Fe and Cr crystals. With the potentials described above, the calculated cohesive energies are 4.01 and 3.84 eV for bcc Fe and Cr, respectively, which is in excellent agreement with the results obtained in Ref. 19, which used the same potentials.

The total binding energy of a defect cluster with n defects can be directly calculated from its formation energy and is defined as the energy difference between the system where all the defects interact and the system where all the defects are far away from each other without any interaction. Thus, the total binding energy for a cluster containing n defects is calculated as

TABLE I. The formation energy, binding energy, and migration energy (eV) for Cr-V clusters and Cr-Fe interstitial in α-Fe.

Configuration	Cr-V (1nn)	Cr-V (2nn)	Cr-V (3nn)	Cr-2V (3nn)	Cr-2V (2nn)	Cr-3V (case I)	Cr-3V (case II)	2Cr-V	Fe-Cr ⟨110⟩
Formation energy (eV)	1.47	1.52	1.43	3.27	2.97	4.52	4.52	1.42	3.12
	1.98[a]	2.02[a]							3.83[a]
Binding energy (eV)	−0.03	−0.08	0.005	−0.11	0.18	0.36	0.36	−0.27	0.12
	0.057[a], 0.082[b] (PAW)	0.014[a]							0.12[b] (PAW)
	0.01[b] (USPP)								0.14[c]
	0.035[b] (EP)								(EP)
Migration energy (eV)	0.56	0.63	0.61	0.67	0.67	0.86	0.89	0.64	0.17
	0.54[a],0.52[d]	0.71[a],0.65[d]							

[a]Reference 18.
[b]Reference 6.
[c]Reference 38.
[d]Reference 19.

$$E_b^{d_1,d_2,\ldots,d_n} = \sum_{i=1}^{n} E_f^{d_i} - E_f^{d_1,d_2,\ldots,d_n}, \quad (2)$$

where $E_f^{d_i}$ is the formation energy of the system containing defect d_i only and $E_f^{d_1,d_2,\ldots,d_n}$ is the formation energy of a defect cluster with n interacting defects.

In the present study of defect migration, several Cr-V clusters and a mixed Cr-Fe interstitial are considered, and first we evaluate their formation and binding energies. The formation energies and binding energies of various defects and defect clusters are listed in Table I, along with the values obtained from *ab initio* and empirical potential (EP) calculations for comparison. The binding energy of a Cr-V pair is small, about −0.03 eV in the first nearest-neighbor (nn) position, and it vanishes at larger separations. The present calculations obtain negative binding energy of a Cr-V cluster, in contrast to the *ab initio* calculations,[18] which is mainly due to the lower formation energy of a Cr substitutional atom (−0.287 eV) compared to that obtained by *ab initio* calculation (−0.12 eV). However, the difference between the present result and all the previous calculations is very small, and does not affect the general migration behavior or energy barrier of a Cr-V cluster (see details below). The cluster binding energy increases as the number of vacancies in the cluster increases but it decreases as the number of Cr atoms increases. This suggests that adding vacancies to the small cluster can stabilize the Cr atoms in the cluster and that adding Cr atoms in the cluster leads to the screening of Cr atoms from each other. The formation energy of a Cr-Fe⟨110⟩ interstitial is calculated to be 3.07 eV, which is smaller than the value of 3.83 eV obtained by *ab initio* calculation.[18]

B. Migration of a Cr-V pair

Both *ab initio*[18] and molecular dynamics[19] calculations revealed that a Cr substitutional atom can diffuse via the vacancy-assisted migration mechanism by directly jumping to the first nearest-neighbor vacancy with a migration barrier of 0.54 eV. From these calculations, it is not clear if a Cr substitutional atom can directly jump to the second and third nearest-neighbor vacancies and how it affects the migration behavior of a nearby Fe atom. In order to get an insight into these detailed migration behaviors, we consider a Cr-V pair containing a single vacancy and one substitutional Cr atom but with different separation distance, i.e., the Cr substitutional atom at the first nearest-neighbor position (1nn) of the vacancy [a and b in Fig. 1], the Cr substitutional atom at the second nearest-neighbor position (2nn) [c and d in Fig. 1] and at the third nearest-neighbor position (3nn) [e in Fig. 1].

Possible migration paths and saddle points are determined by running 100 dimer searches on each initial configuration of a substitutional Cr-vacancy pair. Figure 1 shows the possible migration paths for a Cr-vacancy pair with different initial configurations as discussed above. For example, of the 100 dimer searches for the Cr-V pair in the 1nn configuration, 22 searches converge to saddle points with 0.56 eV. 35 searches converge to other saddle points with 0.66 eV and two searches fail to find saddle points. For the Cr-V pair in the 1nn configuration, the most frequently observed migration mechanism [see Fig. 1(a)] is the Cr atom jumping into the vacancy position [Fig. 1(a)], with the energy of 0.56 eV, which corresponds to the position exchange of the Cr atom and the vacancy. Another mechanism [see Fig. 1(b)] is achieved by a nearby Fe atom jumping to the vacant site, creating a 2nn Cr-V pair. This transition has a higher energy barrier of 0.66 eV. The migration energy barrier for an Fe atom hopping to the nearby vacant site of the Cr atom is comparable to the energy barrier of an Fe hopping in pure Fe, which demonstrates that the effect with the presence of a substitutional Cr on the migration of Fe is rather small. For a Cr-V pair in the 2nn configuration, Fe atoms are at all of the eight first nearest-neighbor positions to the vacancy and the Cr substitutional atom is a second nearest neighbor to the vacancy. The energy barrier for the Cr atom to jump directly to the vacancy position [see Fig. 1(c)] is 2.0 eV, which is 1.44 eV higher than that for the Cr-V(1nn) pair transition. As a consequence, it is unfavorable for the Cr atom to directly jump the second nearest-neighbor vacant site. In this case, the nearby Fe atoms can more easily jump to the vacancy

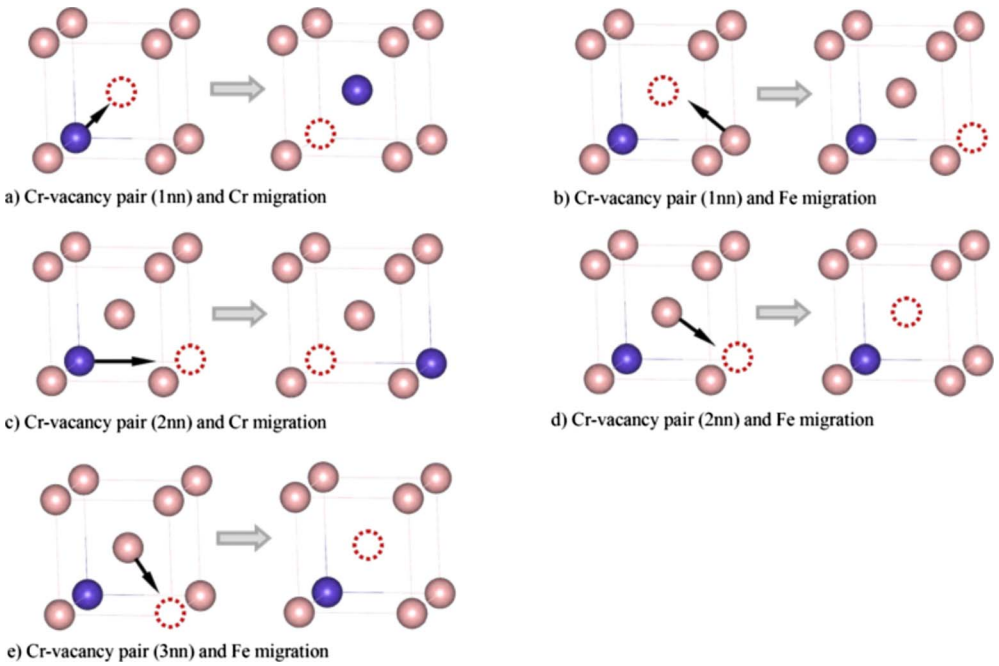

FIG. 1. (Color online) The migration mechanism of a single vacancy and a substitutional Cr atom in a single bcc unit cell. The dashed circle presents the vacancy position at 1nn, 2nn, and 3nn sites. The red and light purple spheres represent the Fe atoms and Cr atoms, respectively. The arrow indicates the migration movement at the next step.

position, as shown in Fig. 1(d), overcoming an energy barrier of only 0.63 eV, which is similar to that for the Cr-V(1nn) pair. Also, for a Cr-V pair in the 3nn configuration the Cr atom directly jumping to the vacancy requires about 2.7 eV, which is more than 2.0 eV higher than that for the Cr-V(1nn) pair. However, as in the case of the Cr-V(2nn) pair, the nearby Fe atoms can jump to the vacancy, and transport the vacancy to create a Cr-V(1nn) pair. The energy barrier for this process obtained from the dimer search is only 0.61 eV, slightly smaller than that for Fe migration. It is of interest to note that the substitutional Cr in α-Fe does not have a significant effect on the migration of Fe atoms at low concentration of Cr. However, it should be pointed out that the long-distance migration of a substitutional Cr atom in Fe requires that Fe transport vacancies to create Cr-V(1nn) pairs, which may require a high concentration of vacancies. It is unlikely that this is a dominant transport mechanism for Cr under normal irradiation conditions in α-Fe.

Once the saddle points for the transitions involved in defect migration are determined, it is possible to trace out the minimum-energy paths using the method described elsewhere.[35] The various energy paths that correspond to the migration processes in Fig. 1 are shown in Fig. 2, where the dash-dotted lines indicate the migration energy barriers of the Cr-V(1nn) pair calculated in Ref. 19. It is obvious that the energy curves of self-diffusion are not symmetric but are lightly distorted, which is affected by the nearby Cr atom. The energy difference between the initial state and final state in Fig. 1(b) is about of 0.03 eV. Note that the saddle point for the Fe atom jump is not at the middle point of the migration path, which is similar to that observed in pure Fe. The middle point of the migration path is a metastable state, at which the energy is 0.57 eV. Overall, the Cr atom overcomes an energy barrier of 0.56 eV, whereas an Fe atom in the same position requires 0.61–0.66 eV for hopping over the energy barriers for a similar transition. The migration energies calculated for the Cr atom in the Cr-V(1nn) pair are in good agreement with the corresponding values of 0.54 and 0.52 eV obtained by *ab initio* methods[18] and empirical potential calculations,[19] respectively.

C. Cr-vacancy clusters

As described above, it is unlikely that a Cr-V pair can lead to long-distance migration of a substitutional Cr. In order to

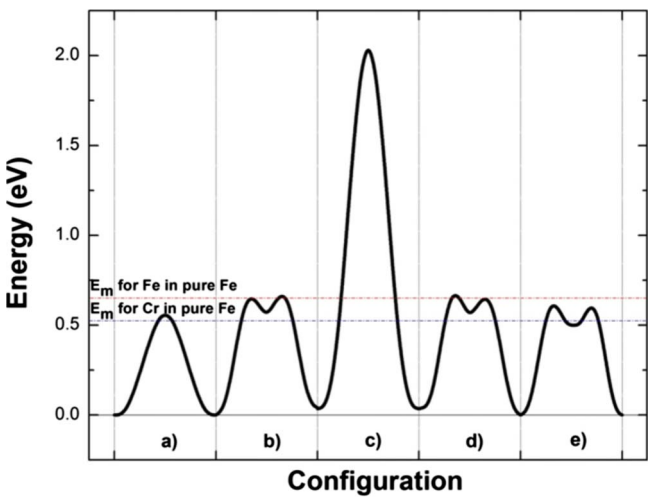

FIG. 2. (Color online) The migration paths of a Cr-V pair, where the reference state is the Cr-V pair at 1nn position. These paths from (a) to (e) correspond to the migration processes shown in Fig. 1. The migration energies calculated in Ref. 19 for Fe and a single Cr atom are given by a red and blue dash-dotted line, respectively.

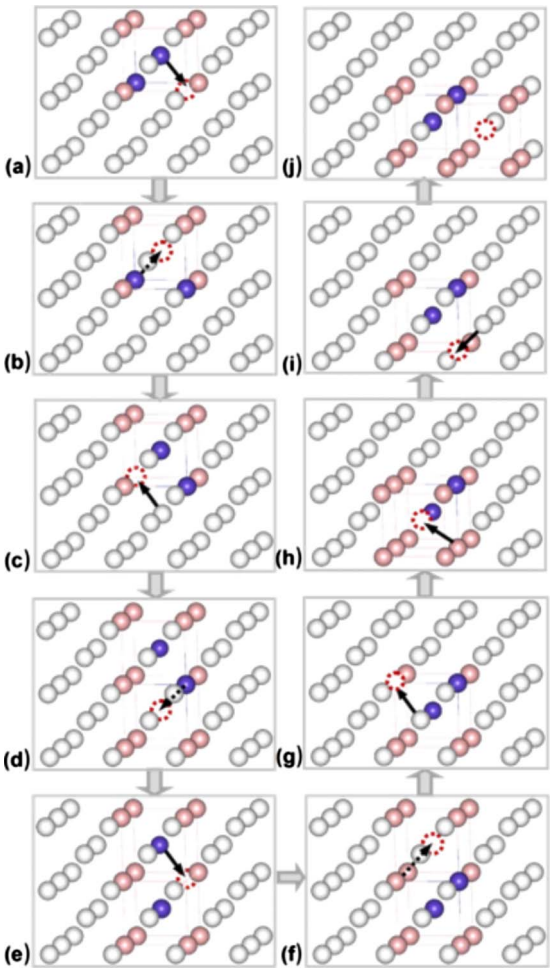

FIG. 3. (Color online) The multistep migration process of a 2Cr-V cluster consisting of two Cr substitutional atoms (blue atoms) and one vacancy (the red dashed circles). In each frame the black arrows indicate the primary atom displacements that result in the atomic arrangement in the next frame.

explore the migration behavior of substitutional Cr, the migration mechanisms of various Cr-V clusters in α-Fe were investigated using the dimer method. The results predict different migration mechanisms than those previously observed in a Cr-V pair and most Cr-V clusters can directly migrate as an object without involving extra vacancies. The first cluster studied is a 2Cr-V cluster that consists of two substitutional Cr atoms and one vacancy nearby. The first atomic configuration in Fig. 3 shows the initial state and 100 dimer searches were carried out to determine the minimum-energy path. The final state of the minimum-energy path is used as the initial atomic configuration for subsequent dimer searches and this process is repeated until a net migration of the cluster is observed. There are ten steps needed to complete a net migration process of the 2Cr-V cluster and the corresponding processes are shown in Fig. 3. Initially, one of the Cr substitutional atoms jumps to the vacant site with an energy barrier of 0.48 eV. In this case, the Cr atom exchanges with the vacancy, following which the other Cr atom moves to the new vacancy site, again overcoming the barrier of 0.48 eV. To complete the net migration process, the 2Cr-V cluster

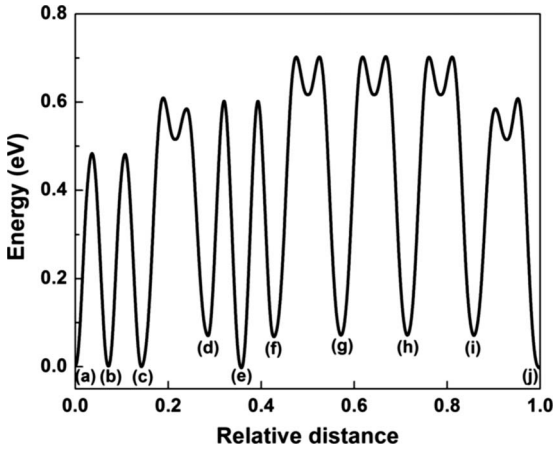

FIG. 4. The migration energy paths of a 2Cr-V cluster, where different paths correspond to the migration processes in Fig. 3, respectively.

needs successive hopping of Fe atoms or substitutional Cr to and from the vacancy. One of the most important features in Fig. 3 is that the 2Cr-V cluster can make a net migration without extra vacancy assistance, which leads to its long-distance migration in the crystal. The migration mechanism is different from the vacancy-assisted migration mechanism observed in the Cr-V pair and it may be defined as a "self-vacancy-assisted" migration mechanism of the cluster. The minimum-energy paths resulting from the migration processes of the 2Cr-V cluster are shown in Fig. 4, where different peaks correspond to the jumps described in Fig. 3. The Cr can directly jump to the vacancy site, whereas the Fe atom needs to pass through a metastable configuration at the middle of the path. The path of Fe jumping is slightly distorted when the Cr is located at the nearest-neighbor distance but it is nearly symmetrical when the Cr is at the second nearest-neighbor site, which suggests that the Cr affect on Fe migration is negligible. Overall, the 2Cr-V cluster needs to overcome an energy barrier of 0.64 eV for its net migration. This energy barrier is similar to that calculated for a Cr-V pair and it may represent one of the preferable mechanisms for the transport of Cr during thermal aging or under irradiation in Fe. However, it should be noted that the binding energy for this cluster is negative, which indicates that this cluster can easily dissociate. The dissociation energy of a vacancy from the 2Cr-V cluster is determined to be 0.66 eV, which equals to the energy barrier for a vacancy to migrate in Fe, but the dissociation energy of a Cr atom the cluster requires much higher energy (i.e., the Cr becomes an interstitial). These results suggest that the net migration energy (0.64 eV) of this cluster is slightly smaller than the dissociation energy (0.66 eV). Thus, this cluster can lead to a long-distance migration without involving extra vacancies.

To further understand the self-vacancy-assisted migration mechanism of the cluster, we have also considered the migration processes of several Cr-V clusters consisting of a single substitutional Cr and two or three vacancies. For a Cr-2V, where two vacancies are in the 2nn position, it takes nine steps to complete a net migration and the corresponding migration processes are shown in Fig. 5. It is clear that the

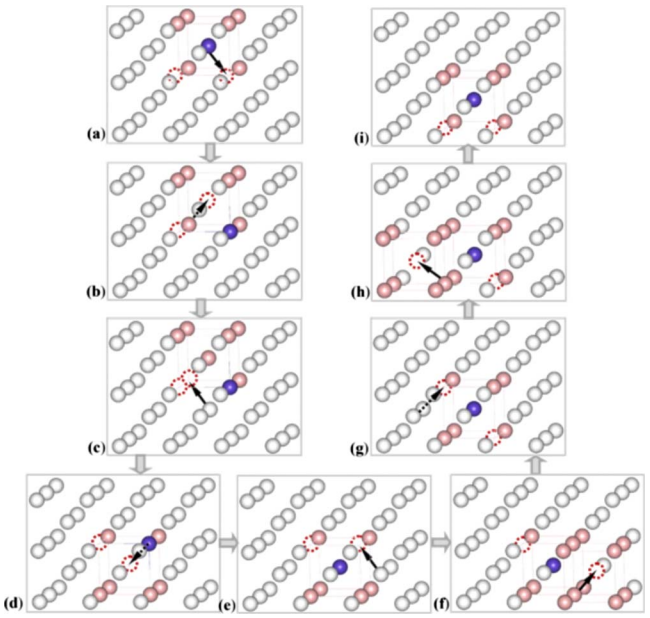

FIG. 5. (Color online) The migration processes of a Cr-2V (2nn) cluster containing one substitutional Cr and two vacancies, where two vacancies are at 2nn positions.

successive hopping of Fe and Cr atoms to the nearby vacancy sites is still a dominant migration mechanism. However, the energy barrier for the Cr and Fe to jump to the vacancy sites in the Cr-2V (2nn) cluster is about 0.02 and 0.05 eV higher than those obtained in the Cr-V (1nn) pair, respectively. The different formation energies of various atomic configurations in the migration process may be attributed to the observed differences of energy barriers. Figure 6 illustrates the minimum migration paths determined from successive dimer searches for the migrating Cr-2V (2nn) cluster. The highest energy barrier in the net migration process (see $c \rightarrow d$ in Figs. 5 and 6) corresponds to the atomic configuration where two 2nn vacancies become 1nn vacancies by the hop of an Fe atom. The atomic configuration, Fig. 5(g), has the largest formation energy of 3.24 eV, as compared to 2.94 eV in the initial state [Fig. 5(a)]. As a result of large differences in formation energies of different configurations as well as different saddle points from different states, the Cr-2V (2nn) cluster needs to overcome the energy barrier of 0.67 eV from $c \rightarrow d$ for a net migration, as shown in Fig. 6. This migration mechanism is similar to that observed for the 2Cr-V cluster, i.e., a self-vacancy-assisted migration mechanism. Thus, the Cr-2V cluster can undergo long-distance migration by itself, a similar feature observed in a 2Cr-V cluster but with a slightly higher migration energy. However, it should be noted that the binding energy of the Cr-2V cluster is negative (−0.11 eV) when the two vacancies are in the third neighbor positions, as shown in Table I. In the migration process, it has appeared that the two vacancies are in the third neighbor position, as seen in Fig. 5(g), and the jump of the vacancies from this position leads the further separation of the two vacancies, as seen in Fig. 5(h). One of the vacancies in Fig. 5(h) can jump away from the cluster but the corresponding energy barrier is found to be 0.65 eV, about 0.28 eV higher than that for the vacancy to jump close to the Cr atom, as shown Fig. 5(i). It is likely that this Cr-2V cluster will be dissociated only at high temperatures.

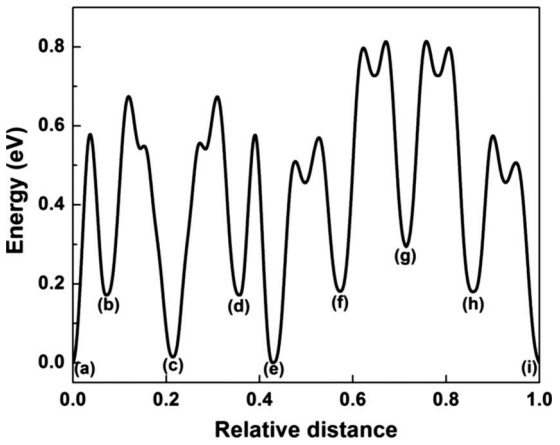

FIG. 6. The migration paths of a Cr-2V (2nn) cluster, where different paths correspond to the migration processes in Fig. 5, respectively. The most stable configuration is shown in Fig. 5(a) with a formation energy of 2.94 eV.

We have also studied a net migration process of a Cr-2V cluster where the two vacancies are initially located as third nearest-neighbor distance. Similar to the migration of the Cr-2V(2nn), the Cr atom and Fe atoms successively jump to vacancy sites, leading to its net migration, and the corresponding migration behavior results in a similar, self-vacancy-assisted migration. However, the Cr-2V(3nn) cluster migration is somewhat less energetically favorable since it is 0.03 eV higher than the Cr-2V(2nn) cluster. This transition is not shown in the figures. The result shows that Cr-2V(3nn) cluster tends to form Cr-2V(2nn) cluster with an energy barrier of 0.61 eV. In this case, it only takes a single Fe jump to the nearest-neighbor site to complete the configuration transformation. The overall migration energy barrier of the Cr-2V(3nn) cluster is dominated by that of the Cr-2V(2nn), i.e., 0.67 eV.

Figures 7 and 8 demonstrate two net migration processes of a Cr-3V cluster with the same initial configuration, one with an Fe hop first (case I) and another with a Cr hop first (case II), respectively. The corresponding minimum-energy paths for these two clusters are shown in Figs. 9 and 10. For the case I, the initial state is not the lowest-energy configuration, and the lowest-energy state is shown in Fig. 7(e), where one of the vacancies jumps to the second nearest-neighbor position of the Cr atom with a formation energy of 4.34 eV. The jump to the next atomic configuration [shown in Fig. 7(f)] requires 0.86 eV, which is the rate limiting step. For the case II, the highest energy state corresponds to the atomic configuration in Fig. 8(f) and the migration energy barrier for this cluster is determined by the jump from the second highest state [Fig. 8(e)], which is also rate limiting. The migration energy barrier is calculated to be 0.89 eV, which is slightly higher than the energy barrier for the case I. The second highest energy configuration for the case II has a formation energy of 4.83 eV, which is 0.34 eV higher than that of the initial configuration.

From the atomic configurations of the various Cr-V clusters, it is clear that the net migration energy for a cluster

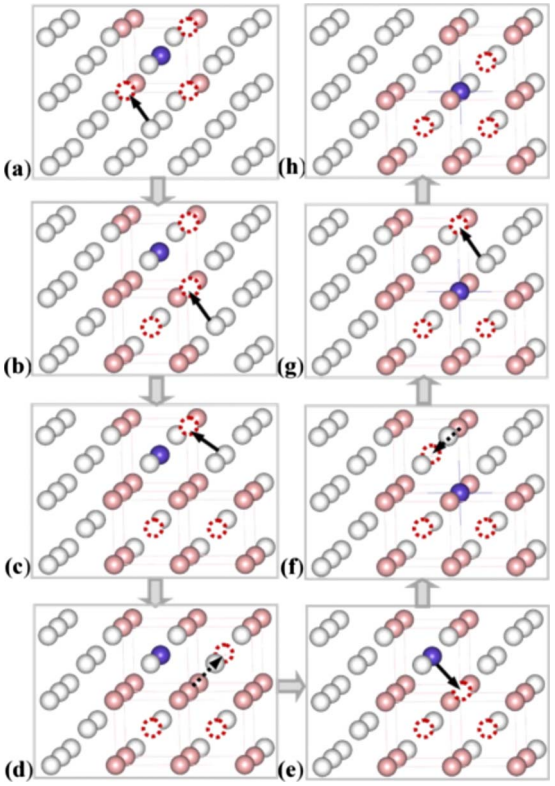

FIG. 7. (Color online) The migration process of a Cr-3V cluster, where the substitutional Cr is located at the top of three vacancies, with Fe hop first.

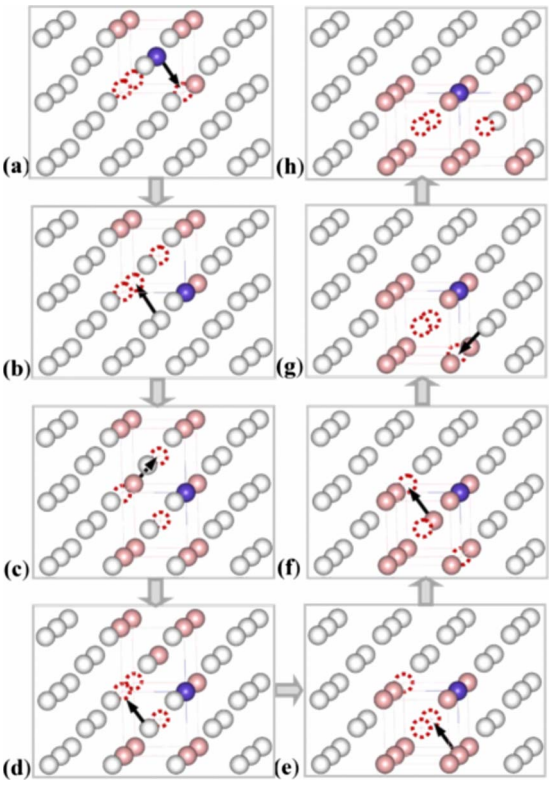

FIG. 8. (Color online) The migration processes of a Cr-3V with a similarly initial configuration but with Cr hop first.

requires that either a Cr or Fe atom jumps to the vacancies in the cluster. Considering that Cr atom has small effect on Fe jumping to nearby vacancies, it is unlikely that a Cr-3V cluster can lead to its long-distance migration in Fe because the migration energy is about 0.25 eV higher than the energy barrier of Fe migration (0.63–0.66 eV). In this case, successive jumps of Fe through vacancies in the cluster can result in the Cr dissociation from the cluster. We have checked the dissociation of the Cr atom from the Cr-3V cluster using the dimer searches and the corresponding energy barrier for this process is about 0.64 eV, which is comparable with that of Fe migration. However, the energy barrier for net migration for Cr-2V or 2Cr-V clusters ranges from 0.64 to 0.67 eV, which is similar to that of Fe migration, and thus, these clusters can lead to their long-distance migration, transporting Cr atoms to other microstructural features. However, it is possible that the Cr atom in these clusters can dissociate from the clusters with similar energy barrier and therefore the competition between Cr dissociation and cluster migration represents a dynamics process of Cr transport in Fe.

D. Mixed ⟨110⟩ interstitials

Both theoretical simulations and experiments predict that the most stable Cr interstitial configuration is the mixed ⟨110⟩ interstitial with an Fe and a Cr atom sharing one lattice site.[18,39–41] Thus, the Cr-Fe⟨110⟩ dumbbell is used as an initial configuration to study interstitial Cr migration. Initially, MD method was used to simulate the diffusion of the Cr-Fe⟨110⟩ interstitial at 600 K and several atomic configurations along the net migration path were quenched to 0 K. Then, the NEB method was used to calculate migration energy barriers. Figure 11 illustrates the migration process of the mixed Cr-Fe⟨110⟩ interstitial, from which it can be seen that several jumps are required to complete a net migration. The Cr atom first changes its orientation from the ⟨110⟩ direction to the $\langle 10\bar{1}\rangle$ direction via a middle atomic configuration shown in Fig. 11(b) and then it jumps to the cubic center position, forming a Cr-Fe$\langle\bar{1}\bar{1}0\rangle$ dumbbell configuration, as demonstrated in Fig. 11(d). Also, the mixed $\langle\bar{1}\bar{1}0\rangle$ interstitial

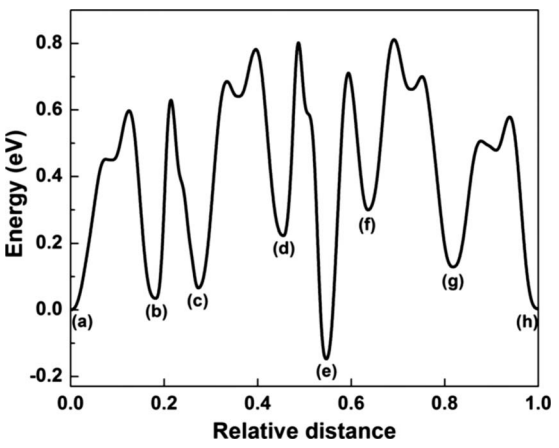

FIG. 9. The migration energy paths of a Cr-3V cluster, where the migration process from $e \rightarrow f$ in Fig. 7 leads to the highest energy barrier.

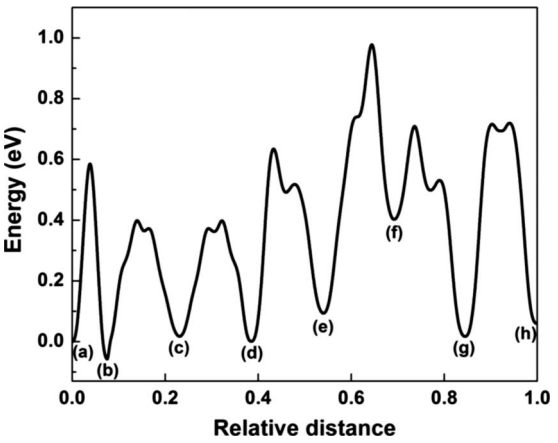

FIG. 10. The migration-energy paths of a Cr-3V, where the highest energy barrier corresponds to the Fe atomic jump from $e \rightarrow f$ in Fig. 8.

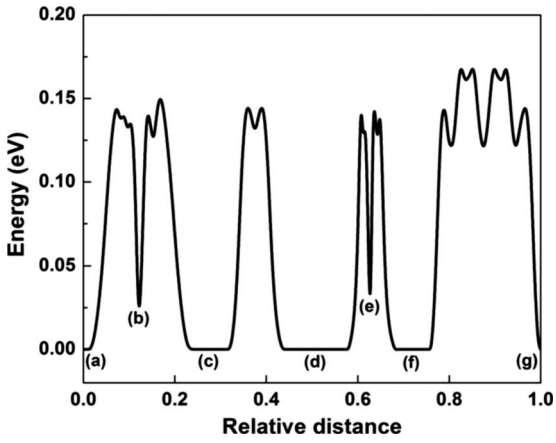

FIG. 12. The migration-energy paths of a Cr-Fe⟨110⟩ interstitial, where the highest energy barrier corresponds to the Fe atomic jump from $f \rightarrow g$ in Fig. 11.

configuration undergoes an on-site rotation, orientating along the $\langle 01\bar{1} \rangle$ direction [Fig. 11(e)], and the Cr in this configuration can directly jump to a first nearest-neighbor position, forming a Cr-Fe⟨101⟩ dumbbell interstitial [Fig. 11(f)]. The on-site rotation of this interstitial completes its net migration and the final configuration is shown in Fig. 11(g). The corresponding energy paths are given in Fig. 12, and the migration energy barrier is determined to be the 0.17 eV and is associated with the on-site rotation. Terentyev *et al.*[38] calculated the migration energies of self-interstitials in dilute and concentrated Fe-Cr alloys by MD simulations with similar interatomic potentials, and found that the stable Cr-Fe dumbbells move faster than vacancies, and they can drag Cr atoms along. The results obtained from the present simulations are in good agreement with their MD simulations. Note that the migration energy of self-interstitial atoms (SIA) in Fe is about 0.31 eV with the current potential but it is only 0.17 eV for a mixed Cr-Fe interstitial. This clearly demonstrates

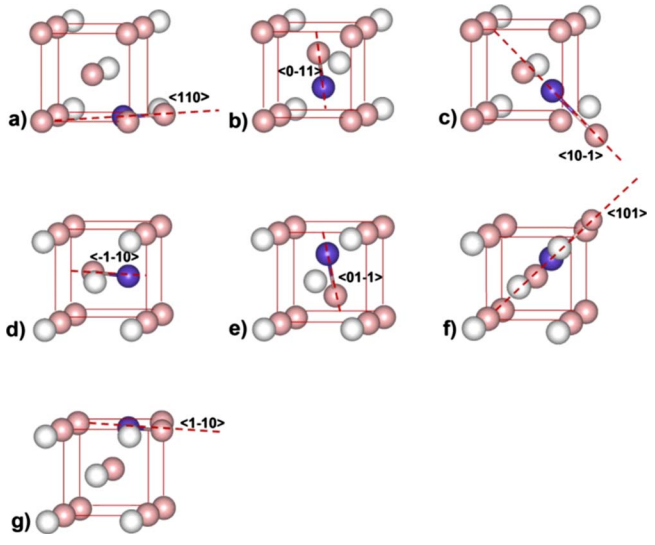

FIG. 11. (Color online) The mixed Cr-Fe⟨110⟩ interstitial migration processes, where the interstitial can migrate via the on-site rotation of the interstitial and Cr atom jump.

that the mixed Cr-Fe interstitial has lower migration energy than a SIA in Fe, which is also consistent with recent density functional theory (DFT) calculations.[17] The slightly faster migration of a mixed Cr-Fe interstitial than an Fe-Fe interstitial in Fe has been suggested in the previous experimental studies.[42,43]

IV. CONCLUSIONS

The dimer method has been employed to study possible transition states of small Cr-V clusters in Fe and thus determine migration mechanisms and minimum-energy paths. The calculations predict that the migration energy of a Cr atom via a vacancy is 0.56 eV, whereas it is about 0.63 eV for an Fe atom in a Cr-V pair, which agrees well with theoretical data for Cr and Fe atom diffusion in pure Fe. The effect of a nearby Cr atom on the migration of Fe is small. However, the migration behavior of a Cr-V pair is unlikely to be a dominate mechanism for transport of Cr under normal experimental conditions in Fe. A series of migration processes for Cr-V clusters in α-Fe was investigated by the dimer searches. It is of interest to find that Cr-2V and 2Cr-V clusters can lead to long-distance migration of Cr, which can be accomplished by Fe and Cr successive jumps to nearby vacancies in the clusters, a mechanism referred to as a self-vacancy-assisted migration. The calculated binding energies of Cr-V clusters show that vacancies weakly attract Cr atoms, and the Cr atom may dissociate from the C-V clusters. Thus, the competition between Cr dissociation and cluster migration represents a dynamics process to transport Cr in Fe.

MD simulations and the NEB method were combined to study the migration behavior of a mixed Cr-Fe interstitial. The results demonstrate that the on-site rotation of the Cr-Fe interstitial requires higher energy than that for its hopping from one site to another and the migration energy is determined to be 0.17 eV, which is lower than that of an Fe SIA. This mixed interstitial migration is believed to be a dominant mechanism for transporting Cr under irradiation in Fe.

ACKNOWLEDGMENTS

This research was supported by a Laboratory Directed

Research and Development Program at the Pacific Northwest National Laboratory, a multiprogram national laboratory operated by Battelle for the U.S. Department of Energy under Contract No. DE-AC05-76RL01830. D.C. and NEAMS under FMM. W.Y.H. were supported by Chinese Academy of Sciences and the National Natural Science Foundation under Contract No. 50671035. The calculations were performed on the supercomputers in the Environmental Molecular Sciences Laboratory, a national scientific user facility sponsored by the Department of Energy, Office of Biological and Environmental Research located at Pacific Northwest National Laboratory.

*Corresponding author. FAX: 1-509 371 6242; fei.gao@pnl.gov

[1] C. H. Woo and B. N. Singh, Philos. Mag. A **65**, 889 (1992).
[2] A. Annenkov, E. Auffray, M. Korzhik, P. Lecoq, and J. P. Peigneux, Phys. Status Solidi A **170**, 47 (1998).
[3] F. Gao, H. Y. Xiao, X. T. Zu, M. Posselt, and W. J. Weber, Phys. Rev. Lett. **103**, 027405 (2009).
[4] F. Tuomisto, K. Saarinen, D. C. Look, and G. C. Farlow, Phys. Rev. B **72**, 085206 (2005).
[5] A. V. Krasheninnikov and K. Nordlund, J. Vac. Sci. Technol. B **20**, 728 (2002).
[6] D. A. Terentyev, L. Malerba, R. Chakarova, K. Nordlund, P. Olssone, M. Rieth, and J. Wallenius, J. Nucl. Mater. **349**, 119 (2006).
[7] L. Malerba, D. Terentyev, P. Olsson, R. Chakarova, and J. Wallenius, J. Nucl. Mater. **329-333**, 1156 (2004).
[8] N. Soneda and T. D. De La Rubia, Philos. Mag. A **78**, 995 (1998).
[9] C. S. Becquart, C. Domain, J. C. van Duysen, and J. M. Raulot, J. Nucl. Mater. **294**, 274 (2001).
[10] F. Garner, M. B. Toloczko, and B. H. Sencer, J. Nucl. Mater. **276**, 123 (2000).
[11] E. A. Little and D. A. Stow, J. Nucl. Mater. **87**, 25 (1979).
[12] D. S. Gelles, J. Nucl. Mater. **108-109**, 515 (1982).
[13] A. Kohyama, A. Hishinuma, D. S. Gelles, R. L. Kluch, W. Dietz, and K. Ehrlich, J. Nucl. Mater. **233-237**, 138 (1996).
[14] S. Brenner, M. Miller, and W. Soffa, Scr. Metall. **16**, 831 (1982).
[15] J. Hyde, A. Cerezo, M. Miller, and G. Smith, Appl. Surf. Sci. **76-77**, 233 (1994).
[16] P. Olsson, I. A. Abrikosov, L. Vitos, and J. Wallenius, J. Nucl. Mater. **321**, 84 (2003).
[17] P. Olsson, J. Nucl. Mater. **386-388**, 86 (2009).
[18] P. Olsson, C. Domain, and J. Wallenius, Phys. Rev. B **75**, 014110 (2007).
[19] P. Olsson, J. Wallenius, C. Domain, K. Nordlund, and L. Malerba, Phys. Rev. B **72**, 214119 (2005); **74**, 229906(E) (2006).
[20] F. Gao, G. Henkelman, W. J. Weber, L. R. Corrales, and H. Jónsson, Nucl. Instrum. Methods Phys. Res. B **202**, 1 (2003).
[21] S. M. J. Gordon, S. D. Kenny, and R. Smith, Phys. Rev. B **72**, 214104 (2005).
[22] E. Meslin, C. C. Fu, A. Barbu, F. Gao, and F. Willaime, Phys. Rev. B **75**, 094303 (2007).
[23] R. J. Kurtz, H. L. Heinisch, and F. Gao, J. Nucl. Mater. **382**, 134 (2008).
[24] D. J. Bacon, F. Gao, and Yu. N. Osetsky, J. Nucl. Mater. **276**, 1 (2000).
[25] D. J. Bacon, A. F. Calder, J. M. Harder, and S. J. Wooding, J. Nucl. Mater. **205**, 52 (1993).
[26] M. J. Caturla, N. Soneda, E. Alonso, B. D. Wirth, T. Díaz de la Rubia, and J. M. Perlado, J. Nucl. Mater. **276**, 13 (2000).
[27] R. E. Stoller, J. Nucl. Mater. **276**, 22 (2000).
[28] W. J. Phythian, R. E. Stoller, A. J. E. Foreman, A. F. Calder, and D. J. Bacon, J. Nucl. Mater. **223**, 245 (1995).
[29] G. J. Ackland, D. J. Bacon, A. F. Calder, and T. Harry, Philos. Mag. A **75**, 713 (1997).
[30] C. S. Becquart, C. Domain, A. Legris, and J. C. van Duysen, J. Nucl. Mater. **280**, 73 (2000).
[31] G. Ackland, M. Mendelev, D. Srolovitz, S. Han, and V. Barashev, J. Phys.: Condens. Matter **16**, S2629 (2004).
[32] A. F. Calder, D. J. Bacon, A. V. Barashev, and Yu. N. Osetsky, J. Nucl. Mater. **382**, 91 (2008).
[33] T. Seletskaia, Yu. N. Osetsky, R. E. Stoller, and G. M. Stocks, J. Nucl. Mater. **351**, 109 (2006).
[34] F. Willaime, C. C. Fu, M. C. Marinica, and J. Dalla Torre, Nucl. Instrum. Methods Phys. Res. B **228**, 92 (2005).
[35] C. Björkas, K. Nordlund, L. Malerba, D. Terentyev, and P. Olsson, J. Nucl. Mater. **372**, 312 (2008).
[36] G. Henkelman and H. Jónsson, J. Chem. Phys. **111**, 7010 (1999).
[37] G. Henkelman and H. Jónsson, J. Chem. Phys. **113**, 9978 (2000).
[38] D. Terentyev, P. Olsson, T. P. C. Klaver, and L. Malerba, Comput. Mater. Sci. **43**, 1183 (2008).
[39] V. Hivert, R. Pichon, H. Bilger, P. Bichon, J. Verdone, D. Dautreppe, and P. Moser, J. Phys. Chem. Solids **31**, 1843 (1970).
[40] A Möslang, H. Graf, G. Balzer, E. Recknagel, A. Weidinger, Th. Wichert, and R. I. Grynszpan, Phys. Rev. B **27**, 2674 (1983).
[41] R. A. Johnson, Phys. Rev. **134**, A1329 (1964).
[42] F. Maury, P. Lucasson, A. Lucasson, and F. Faudot, J. Phys. F: Met. Phys. **17**, 1143 (1987).
[43] H. Abe and E. Kuramoto, J. Nucl. Mater. **271-272**, 209 (1999).